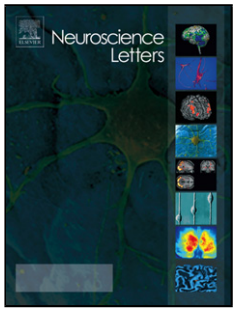

Title: Neural correlates of decision making on whole body yaw rotation: an fNIRS study

Author: K.N. de Winkel A. Nesti H. Ayaz H.H. B*ü*lthoff

PII: S0304-3940(17)30365-8
DOI: http://dx.doi.org/doi:10.1016/j.neulet.2017.04.053
Reference: NSL 32794

To appear in: *Neuroscience Letters*

Received date: 12-12-2016
Revised date: 12-4-2017
Accepted date: 26-4-2017

Please cite this article as: K.N. de Winkel, A. Nesti, H. Ayaz, H.H. B*ddotu*lthoff, Neural correlates of decision making on whole body yaw rotation: an fNIRS study, *<![CDATA[Neuroscience Letters]]>* (2017), http://dx.doi.org/10.1016/j.neulet.2017.04.053

Neural correlates of decision making on whole body yaw rotation: an fNIRS study

K.N. de Winkel, A. Nesti, H. Ayaz, H.H. Bülthoff

June 12, 2017

Prominent accounts of decision making state that decisions are made on the basis of an accumulation of sensory evidence, orchestrated by networks of prefrontal and parietal neural populations. Here we assess whether these findings generalize to decisions on self-motion.
Participants were presented with whole body yaw rotations of different durations in a 2-Interval-Forced-Choice paradigm, and tasked to discriminate motions on the basis of their amplitude. The cortical hemodynamic response was recorded using functional near-infrared spectroscopy (fNIRS) while participants were performing the task.
The imaging data was used to predict the specific response on individual experimental trials, and to predict whether the comparison stimulus would be judged larger than the reference. Classifier performance on the former variable was negligible. However, considerable performance was achieved for the latter variable, specifically using parietal imaging data. The findings provide support for the notion that activity in the parietal cortex reflects modality independent decision variables that represent the strength of the neural evidence in favor of a decision. The results are encouraging for the use of fNIRS as a method to perform neuroimaging in moving individuals.

1 Introduction

Decision making is an essential mental process of intellectual functioning, and represents a component of higher order cognition. According to prominent accounts of the decision making process[1, 2], sensory evidence is accumulated over time to reduce noise and evade ambiguity. Specifically, noisy information provided by our sensory modalities is integrated into a decision variable (DV) incrementally. This DV reflects sensory evidence in favor of particular hypotheses, and decisions are reached when the evidence reflected in the DV crosses some internal bound.
Consistent with this notion, [3] found that decisions made by human participants on heading of self-motion reflected an accumulation of evidence over time. Similarly, in

previous work by our group [4], we obtained behavioral evidence that the Central Nervous System (CNS) accumulates sensory evidence on rotatory self-motion over time. In this study, participants seated on a motion platform were rotated in a sinusoidal fashion around an Earth-vertical yaw axis, and instructed to discriminate two consecutive motions on the basis of their amplitude. The results showed that the ability to tell two consecutive rotations apart improves asymptotically as the duration of the individual motion stimuli was increased from one to five seconds. Given that stimulus duration was increased simply by increasing the number of cycles of rotation, while the frequency of the motion profiles was kept constant, these results indicate that sensory evidence on physical rotations is indeed accumulated over time.

Single cell recordings in rats and monkeys have yielded neural correlates of sensory evidence and DVs in the prefrontal and parietal lobes [5, 6, 2, 7, 8, 9, 10], and electrophysiological recordings in humans have revealed a positivity in the Electro-Encephalogram (EEG) that bears the characteristics of a modality-independent DV [11, 12]: the amplitude of this signal scales with the strength of the sensory evidence, and it exhibits a threshold relationship to responses, which means a response is typically observed after the signal exceeds a certain threshold. Moreover, the signal was identified regardless whether a visual or auditory decision task was performed, suggesting that these reflections of DVs are modality-independent.

In the present study, we investigated whether the findings on neural correlates of DVs in prefrontal and parietal cortical areas generalize to decision making based on perceptions of self-motion.

Neuroimaging data on self-motion perception is scarce, because most imaging equipment cannot be used with moving participants: rotatory motion of the head induces reflexive eye-movements such as the vestibulo-ocular reflex that introduce artifacts in EEG signals, thereby limiting the usability of the data [13]; and whole body motion in current fMRI scanners is impossible. We therefore opted to use functional near-infrared spectroscopy (fNIRS, e.g., [14, 15, 16]). fNIRS makes use of the fact that tissues other than hemoglobin are mostly transparent to near-infrared light. By locally applying near-infrared light of two different wavelengths and measuring scattering and absorption, changes in the concentrations of oxygenated (HbO_2) and deoxygenated (HbR) hemoglobin can be calculated, revealing changes in the blood volume in that area. Changes induced by exposure to a stimulus are known as the hemodynamic response (HR, [17]). We looked for neural correlates of decision making on self-motion in recordings of the HR measured over the prefrontal and parietal areas. The experimental paradigm was adapted from [4]. Rather than presenting experimental conditions in random order, we presented conditions in blocks to accommodate requirements on the experimental design imposed by fNIRS.

Based on our previous behavioral findings, we hypothesized that the ability to discriminate whole body yaw-rotations improves for longer duration motions. Furthermore, we hypothesized that characteristics of the HR, as recorded over the prefrontal and/or parietal lobes, reflect task performance, and that differences in performance for motions of different durations are associated with differences in the characteristics of the HR.

2 Methods

2.1 Ethics statement

The experiment was performed in accordance with the declaration of Helsinki. The experimental protocol was approved by the ethical commission of the medical faculty of the Eberhard-Karls University in Tübingen, Germany, reference number 714/2016BO2.

2.2 Participants

Seventeen people took part in the experiment. 15 naive participants were recruited from the institute participant pool; the two remaining participants were experimenters KW and AN. For nine participants (three female), activity was recorded over the prefrontal lobe (detailed below). The average age of these participants was 24.8 years, with a standard deviation of 3.6 years. Activity was recorded over the parietal lobe for eight other participants (three female). The average age in this group was 29.6 years, with a standard deviation of 2.1 years.
In accordance with motion platform safety requirements, participation was limited to people measuring at most 1.95m long, and weighing under 100kg; people with a (history of) vestibular illness, spinal problems, heart or circulatory disease, a heart pacemaker, and pregnant women were also excluded from participation.

2.3 Setup

Motion stimuli were presented using an eMotion 1500 hexapod motion system (Bosch Rexroth AG, Lohr Am Main, Germany), capable of producing yaw rotations with a range of 54°, and a maximum velocity of 41°/s. The platform was controlled using MATLAB Simulink software (The MathWorks, Inc., Natick, Massachusetts, United States).
Participants were seated in an automotive style bucket seat (RECARO GmbH, Stuttgart, Germany) that was mounted on top of the platform, and secured with a 5-point safety harness (SCHROTH Safety Products GmbH, Arnsberg, Germany). To minimize head movements, participants also wore a philadelphia type cervical collar.
To mask the sounds of the motion platform, participants wore earplugs with a 33dB signal-to-noise ratio (Honeywell Safety Products, Roissy, France) as well as a wireless headset (Plantronics, Santa Cruz, California, United States) that actively canceled outside noise, and that also played white noise during stimulus presentation.
The neuroimaging equipment (detailed in section: Neuroimaging) and the computer used to control this equipment and record the data were mounted to the motion platform.
Participants provided their responses to the experimental task using an Xbox wireless controller (Microsoft, Redmond, Washington, United States). A photograph of the setup is provided in Figure 1.

Figure 1: Photograph of the motion platform. The fNIRS equipment is not pictured.

2.4 Task

Participants performed a 2-Interval Forced Choice task (2IFC). On each experimental trial, participants were presented with two successive full body rotations around a vertical yaw-axis (i.e., stimuli), separated by a 2s break. One of these rotations had a fixed amplitude of 15°/s and was designated *reference*; the other rotation had an amplitude chosen from a range around the reference and was designated *comparison*. Reference and comparison stimuli were presented in random order on individual trials. Participants were tasked with judging which stimulus of the pair had the larger amplitude (i.e., 'first' or 'second').

2.5 Stimuli

Each stimulus had the following profile in angular velocity ω:

$$\omega = A\sin(2\pi f t), \tag{1}$$

with $f = 0.5$Hz. Experimental conditions were defined by varying the amplitude A of the comparison stimulus and the duration of the motion stimuli. The comparison levels were $A_{\text{comparison}} = [10.00, 11.25, 12.50, 13.75, 16.25, 17.50, 18.75, 20.00]$°/s. Duration of the stimuli was varied by presenting either 0.5, 1, or 1.5 cycles (n_{cycles}) of the sinusoid, corresponding to motions of one, two, and three seconds each, respectively. A schematic illustration of experimental trials is available as Supplementary Material Figure S1.
In order to avoid floor-effects in the behavioral task, randomly generated heave vibrations were added to the motion stimuli [18, 19, 20, 21]. Vibrations were in the range of 4-8 Hz and had a Root Mean Square (RMS) value of approximately 0.1m/s^2, comparable to rumble experienced driving a car on a bumpy road. These vibrations were present from 1s prior to the onset of the first motion stimulus to 1s after the offset of the last stimulus.
Each experimental condition was presented 15 times. In total, each participant completed $3(n_{\text{cycles}}) \times 8(A_{\text{comparison}}) \times 15(\text{repetitions}) = 360$ experimental trials.

2.6 Neuroimaging

We recorded the HR using a Brain Products NIRSport Model 88 mobile imaging system (Brain Products GmbH, Gilching, Germany). The NIRSport performs continuous-wave near-infrared diffuse tomographic measurements on wavelengths of 760 and 850nm, with a sampling rate of 7.8125Hz. The device features eight near-infrared LED sources and eight detectors. Sources and detectors are arranged in a grid to form 'optodes'; the signal from each optode reflects hemodynamic activity centered between the corresponding source-detector pair. As a rule of thumb, measurements reveal activity at a tissue depth of about half the source-detector distance. We used the international 10-10 EEG system (e.g., [22]) as a reference for source-detector placement, which allowed us to space sources and detectors approximately 30mm apart. Given that the human cranium has a thickness of 5.4-8.2mm[23], arrangements using this reference system should provide

sufficient depth to reveal cortical hemodynamics.
The HR was measured over two regions of interest: over the prefrontal area for nine participants, and over the parietal area for eight others (Figure 2). A headband provided with the NIRSport-88 was used to record over the prefrontal area; a NIRScap (Brain Products GmbH, Gilching, Germany) was used to set up a grid over the parietal area.

(a) (b)

Figure 2: Illustration of frontal (left panel) and parietal (right panel) recording layouts. White dots illustrate the optodes formed by a certain source (red) and detector (green), as they are defined in the main text.

The 22 prefrontal optodes on the headband correspond, approximately, to the following locations of the 10-10 EEG system: 'FC3-F5', 'FC3-F1', 'AF7-F5', 'AF7-Fp1', 'AF3-F5', 'AF3-F1', 'AF3-Fp1', 'AF3-AFz', 'Fz-F1', 'Fz-AFz', 'Fz-F2', 'Fpz-Fp1', 'Fpz-AFz', 'Fpz-Fp2', 'AF4-AFz', 'AF4-F2', 'AF4-Fp2', 'AF4-F6', 'FC4-F2', 'FC4-F6', 'AF8-Fp2', 'AF8-F6'. The layout is visualized in Figure 2a
The parietal-layout provided the following 23 optodes: 'C1-CP1', 'C1-Cz', 'CP3-CP1', 'CP3-P3', 'P1-CP1', 'P1-P3', 'P1-PO3', 'P1-Pz', 'CPz-CP1', 'CPz-Pz', 'CPz-Cz', 'CPZ-CP2', 'POz-PO3', 'POz-Pz', 'POz-PO4', 'P2-Pz', 'P2-PO4', 'P2-CP2', 'P2-P4', 'C2-Cz', 'C2-CP2', 'CP4-CP2', 'CP4-P4'. The layout is visualized in Figure 2b.

2.7 Procedure

In previous work, task related changes in HbR and HbO_2 concentrations in response to task specific conditions, have been shown to become apparent from analysis of prolonged recordings rather than brief intervals (e.g., [24]). We therefore decided to present the 15 trials from each specific condition in three blocks: of four, five and six trials. This procedure allowed us to keep the task requirements constant for a prolonged length of time, and thereby allow both a trial and block based analysis. The blocks were presented in a random order, with the constraint that blocks of any specific condition were not presented directly after another, which would essentially result in a longer block. The median duration of the blocks was $68.2, 64.4, 85.7$s for blocks of four, five, and six trials respectively. Variability in block-duration was due to participants pacing trial presentation themselves.
The experiment was divided into two separate sessions, performed on two consecutive days. The sessions were approximately equal in the number of trials presented (180 ± 2, due to block length) and overall duration, lasting between $1.5 - 2$ hours, including 15-30 minutes set-up time of the neuroimaging equipment.

2.8 Data analyses

2.8.1 Analyses of behavioral data

The probability that a participant judges the comparison stimulus to be more intense than the reference stimulus varies as a function of comparison stimulus amplitude $A_{\text{comparison}}$. This was modeled by fitting the binary response variable R with a cumulative normal distribution function (Φ):

$$\mathrm{P}(R) = \lambda_s + (1 - 2 * \lambda_s)\Phi\left(\frac{A_{\text{reference}} - A_{\text{comparison}}}{\sigma_{n_{\text{cycles}}}}\right) \quad (2)$$

Here $\sigma_{n_{\text{cycles}}}$ are slope parameters that reflect discriminatory ability for the different levels of the number of cycles factor, $n_{\text{cycles}} = 0.5, 1.0, 1.5$. These parameters will be referred to as Just-Noticeable Difference (JND) for consistency with the psychometric literature (e.g., [25, 21]). Lapse rate parameters λ_s were also included in the model to account for momentary lapses of attention[26]. The lapse rate was allowed to vary between experimental sessions ($s = 1, 2$), to allow for changes in attention between consecutive days of experimental testing, and was limited to values between 0 and 0.05. Fitting was performed for data of each participant individually, using the method of Maximum-Likelihood[27].

Based on previous results[4], the value of the slope parameter was expected to decrease as the number of cycles is increased, reflecting accumulation of evidence. This hypothesis was tested by assessing whether the estimated JNDs differed between the levels of n_{cycles}, and if so, whether the JND decreased consistently as n_{cycles} was increased. Specifically, we fitted the following mixed-effect model (in Wilkinson-notation[28]):

$$\text{JND} \sim 1 + n_{\text{cycles}} + (1|\text{pp}) \quad (3)$$

here (1|pp) represents a random intercept for different participants. n_{cycles} was treated as a categorical variable. All analyses were performed using MATLAB R2014b (The MathWorks, Inc., Natick, Massachusetts, United States).

2.8.2 Analyses of neuroimaging data

For each participant, fNIRS recordings for the two different experimental sessions were concatenated, and filtered using a 3rd order bandpass filter with cut-off frequencies of 0.01 and 0.3Hz to remove unwanted signals such as heart-rate (similar to e.g., [29]).

Two sets of epochs were cut. One set of epochs contained recordings from the beginning until the end (the moment the last response was given) of each experimental block; the other set contained epochs for each individual trial, from trial-onset to 12 seconds later. This length was chosen because a typical HR lasts approximately this long[30]. It should be noted that when the duration of a trial was under 12 seconds, the end of trial-epochs partly reflects the HR associated with a subsequent trial. This procedure may introduce additional noise into the trial-based analyses.

Each epoch was baseline-corrected by subtracting the first measurement value from the

entire epoch, and four metrics were calculated; the mean, maximum, Root Mean Square (RMS), and the Area Under Curve (AUC). The metrics were calculated for HbTotal, which was defined as the sum of the HbO_2 and HbR recordings.

A number of analyses was performed for each metric in both sets: first, we assessed whether the value of either metric, for convenience denoted y, in any specific optode i was affected by the experimental manipulations in a systematic way. To do so, we fitted the following mixed-effect models for trial and block data, respectively:

$$y_i \sim 1 + n_{\text{cycles}} * A_{\text{comparison}} + (1|\text{pp}) \tag{4}$$

and

$$y_i \sim 1 + n_{\text{cycles}} * A_{\text{comparison}} + n_{\text{block}} : n_{\text{cycles}} + (1|\text{pp}), \tag{5}$$

where n_{cycles} and n_{block} represent fixed effects for the number of cycles and number of trials in a block, and (1|pp) indicates a random effect (intercept) for participant pp. The interaction between n_{cycles} and n_{block} was included in the block-based analyses to account for potential confounding effects of differences in the length of epochs. All independent variables were treated as categorical predictors. Bonferroni corrections for multiple comparisons were performed.

Second, we assessed whether task performance was related to activity in any specific optode, by calculating correlations between the JNDs and average values of each of the metrics (averaged over participants), for each optode individually.

Lastly, we investigated whether the recorded activity in any (combination of) optodes could predict responses on an individual basis. More specifically, we performed two analyses: in the first analysis, logistic regression models were fitted to the binary response variable (i.e., 'first' or 'second'), with the mean-metrics calculated for each optode as potential predictors; in the second analysis, the same type of models were fitted to the binary variable reflecting that participants had judged the comparison stimulus to be larger than the reference stimulus[1]. To determine which optode(s) contained information on these variables, we fitted the models in a stepwise fashion, using the 'stepwiseglm' routine in MATLAB (The MathWorks, Inc., Natick, Massachusetts, United States). The algorithm starts out with a model containing only an intercept, and incrementally adds/removes optodes based on improvement of the models Akaike Information Criterion (AIC)-score. The algorithm terminates when no single step improves the AIC score. The largest terms allowed were linear. To assess the performance of the fitted models, we predicted the probabilities of positive responses for all trials using leave-one-out cross validation procedures, and used these predictions to generate Receiver Operating Characteristic (ROC) curves[31].

[1]For each trial, the models provide a prediction of the probability of a positive response, which we defined as 'comparison larger than reference', and 'second', for the two different analyses. The complement of the predicted probability is the model's prediction on the alternative response (i.e., 'comparison is smaller than reference', and 'first')

3 Results

The results of the experiment are presented in two parts. The first part summarizes the analysis of behavioral data. We assessed whether the ability to discriminate yaw-rotations on the basis of the motion's amplitude varies with stimulus duration. The second part consists of an analysis of the neuroimaging data, which was aimed at identifying neural correlates of the behavioral data.

3.1 Behavioral results

The ability to discriminate between motion stimuli was operationalized as the JND (see section: Analyses of behavioral data). We tested whether the estimated JNDs differed between the levels of n_{cycles}, but a statistical analysis did not reveal any difference between the levels of n_{cycles} ($F(2, 48) = 2.34, p = 0.11$). A summary of the JNDs for the different levels of n_{cycles} is presented in Supplementary Material Figure S2.

3.2 Neuroimaging results

Recordings over the parietal cortex yielded HRs that closely resembled the typical response reported in the literature[30]; recordings over the prefrontal cortex generally yielded less distinctive peakedness. Figures showing the HR to all experimental conditions are provided as Supplementary Material Figures S3-S5 for frontal sites and in Figures S6-S8 for parietal sites.

Apart from the difference in shape of the signal, the HR was also stronger over the parietal area than over the prefrontal area: the mean, maximum, RMS, and AUC metrics of the trial-epochs were all larger for the parietal recordings (respectively, $\mathrm{F}(1, 1.37\times10^5) = [18.28, 15.94, 7.07, 18.33], p = [1.91 \times 10^{-5}, 6.53 \times 10^{-5}, 7.83 \times 10^{-3}, 1.86 \times 10^{-5}]$). The average values of the metrics per location are presented in Supplementary Material Table S1. We tested whether experimental manipulations affected the HR in prefrontal and/or parietal locations in any consistent fashion by modeling the mean, maximum, RMS, and AUC metrics as functions of the experimental manipulations. These analyses were run for the set of epochs corresponding to blocks of trials, as well as for the set of epochs corresponding to individual trials (see section: Analyses of neuroimaging data). There were no significant effects that were consistent among metrics, and/or that held up after correction for multiple comparisons.

Task-performances, operationalized as JNDs, did not correlate with metrics recorded in specific optodes. These results were not different depending on whether analyses were performed on trial or block data.

Tables with the results of the statistical tests and correlations presented above are available as Supplementary Material Tables S2-S5.

Finally, we fitted logit-models on an individual basis to assess whether the fNIRS recordings from idiosyncratic subsets of optodes could predict specific responses (i.e., 'second' or reciprocally, 'first'), and/or whether the response reflected that the comparison stimulus had been judged more intense than the reference (see section: Analyses of neu-

roimaging data). To evaluate model performance, we constructed ROC curves. ROC curves show how the true vs. false positive rate of predictions based on model output varies as the criterion for a positive response varies from liberal to conservative. The area under the ROC curve (AUROCC) is an indicator of model performance, where values of 0.5 indicate that the model does not perform any better than chance, and a value of 1 indicates perfect classification. An exemplary ROC curve is presented in Supplementary Material Figure S9.

The results of the fitting procedure for the prediction of specific responses ('first' or 'second') are presented in Table 1. Models using frontal optodes performed better than chance for five out of nine participants; models using parietal optodes did so for seven out of eight participants. There was considerable variability between participants in which specific optodes were included in the final models by the stepwise regression procedure (see Supplementary Material Document S1). A comparison of AUROCC values using a Mann-Whitney rank-sum test indicated no difference in model performance between recording sites (W=41, $p = 0.673$).

Table 1: Evaluation of logit models for the binary response variable. n_o represents the number of optodes included in the final model, p is the probability of an intercept-only model over the final model (significant fits are boldfaced), and the AUROCC is the area under the ROC curve.

prefrontal				parietal			
participant	n_o	p	AUROCC	participant	n_o	p	AUROCC
1	1	0.051	0.542	1	3	**0.001**	0.604
2	1	0.066	0.536	2	3	**0.004**	0.535
3	2	0.121	0.536	3	1	0.146	0.512
4	5	**0.002**	0.613	4	2	**0.015**	0.551
5	1	0.083	0.511	5	2	**0.001**	0.593
6	2	**0.024**	0.552	6	3	**0.004**	0.578
7	2	**0.034**	0.557	7	6	**0.000**	0.603
8	5	**0.003**	0.590	8	1	**0.040**	0.529
9	1	**0.036**	0.514				
median	2	0.036	0.542	median	2.5	0.004	0.565

For predictions on whether the comparison stimulus would be judged larger than the reference, the model fitting results are presented in Table 2.

Here, the models performed better than chance in all cases. Again, there was considerable variability between participants in which specific optodes were included in the final models (see Supplementary Material Document S1). A comparison of AUROCC values using a rank-sum test indicated better performance for models using parietal recording sites as predictors than for models using frontal recording sites as predictors (W=59, $p = 0.027$). Pairwise Wilcoxon signed-rank tests revealed that the observed AUROCC values were significantly higher when predicting whether the comparison stimulus would be judged more intense than the reference, than when predicting specific responses, for

Table 2: Evaluation of logit models for responses reflecting that the comparison stimulus was judged more intense than the reference. n_o represents the number of optodes (and interactions) included in the final model, p is the probability of an intercept-only model over the final model (significant fits are boldfaced), and the AUROCC is the area under the ROC curve.

prefrontal				parietal			
participant	n_o	p	AUROCC	participant	n_o	p	AUROCC
1	6	**0.002**	0.591	1	7	**0.000**	0.710
2	4	**0.004**	0.589	2	6	**0.003**	0.598
3	6	**0.002**	0.578	3	8	**0.000**	0.707
4	5	**0.003**	0.598	4	5	**0.000**	0.632
5	6	**0.004**	0.556	5	2	**0.013**	0.592
6	8	**0.000**	0.643	6	7	**0.000**	0.645
7	4	**0.001**	0.622	7	3	**0.000**	0.627
8	8	**0.000**	0.623	8	6	**0.000**	0.620
9	5	**0.002**	0.596				
median	6	0.002	0.596	median	6	0.000	0.629

both frontal (V=44, $p = 0.008$) and parietal recordings (V = 35, $p = 0.016$).

4 Discussion

The present study was designed to assess whether neural correlates of decision making on self-motion could be extracted from fNIRS recordings of cortical hemodynamic activity. Based on the literature, we identified two regions of interest: the prefrontal cortex, which has been attributed a central role in decision making[32, 33, 34], reflecting for example specific decisions[9] and the quality of the decision making process under ambiguity and risk[35, 36, 37, 38]; and the parietal cortex, which is thought to reflect the sensory evidence gathered on alternative decisions[7, 12, 8, 9, 10]. On the basis of previous behavioral results[3, 4], we hypothesized that decision making would improve for longer duration stimuli due to an accumulation of evidence. Moreover, we hypothesized that characteristics of the hemodynamic response would reflect decision making and an accumulation of evidence.

A substantial literature exists on what is known as path integration, which refers to an ability to navigate through the environment purely on the basis of inertial information (i.e., vestibular and somatosensory). This ability has been demonstrated to be present in many animals, including humans (e.g., [39, 40, 41, 42]). The presence of this ability in an animal indicates that the animal is able to update a position estimate by integrating transient inertial information, thus accumulating sensory evidence. In contrast to the findings of a previous study by our group[4], accumulation of evidence was not apparent from the present behavioral data. This is surprising, because the present study employed essentially the same experimental paradigm, with the exception that trials

of specific conditions were presented in three blocks per condition instead of in a completely randomized order. This difference however does not readily explain the difference in findings: none of the participants noticed that trials were presented in blocks, and the presentation order of comparison and reference stimuli within trials was random. We do not contend that sensory evidence on self-motion is *not* accumulated over time; this is unlikely given that many animals are able to perform path integration. Rather, we speculate that any benefits of an accumulation of evidence were negated by the need to keep a fleeting internal representation of a longer duration stimulus in short-term memory for longer.

In line with the absence of effects in the behavioral data, recordings of hemodynamic activity in neither prefrontal nor parietal optodes were affected by stimulus duration, regardless whether the existence of such effects was assessed from epochs corresponding to individual trials or experimental blocks. The HR also did not vary with the amplitude of the comparison stimulus in any consistent fashion. It is interesting to note that given the absence of behavioral effects of the motion characteristics, the absence of effects of the motion characteristics on the neuroimaging data allows us to exclude the possibility that the motions introduced systematic noise in the fNIRS data. Moreover, the absence such effects indicates that the present neuroimaging data do not reflect processing of a motion characteristic per se, for which the parietal cortex has been implicated previously (e.g., [43, 44]).

In further evaluation of relations between the behavioral and neuroimaging data, we assessed whether the JNDs correlated to the value of the metrics in specific channels, but found this not to be the case. However, this approach only assesses whether there are commonalities between participants in how the value of metrics in specific optodes affect performance; it is not suitable to assess whether there is a relationship between the pattern of activity in subsets of optodes and characteristics of the choices made on individual trials. We therefore also assessed whether metrics obatined from subsets of optodes could be used simultaneously to predict the specific response on individual trials and/or whether or not this response reflected that the comparison stimulus had been judged to be more intense than the reference. More specifically, we used a stepwise approach to fit logistic regression models that predicted the probability of positive responses, respectively corresponding to: 'second stimulus is more intense', and 'comparison is larger than reference'.

With respect to the prediction of specific responses, the performance of the fitted models could not be distinguished from guessing for five out of seventeen participants, and could be considered poor in the other cases, given that the AUROCC was generally below 0.6. These results did not differ between recording sites.

Better results were achieved when predicting whether or not the comparison stimulus was judged larger than the reference. Here, the models performed significantly better than guessing in all cases, and AUROCC values were significantly higher than the values observed for prediction of specific responses, for both recording sites. Moreover, models using parietal recordings provided significantly better predictions (median AUROCC = 0.629) than models using prefrontal recordings (median AUROCC = 0.596). This latter finding is consistent with the finding that signals recorded over the prefrontal cortex

were weaker.

Although it should be noted that only a small group of participants were tested, the findings of this study provide support for the notion that activity in the parietal cortex reflects modality independent DVs that represent the strength of the evidence in favor of a decision[7, 12, 8, 9, 10]. Overall, the present results are encouraging for the use of fNIRS as a modality to perform neuroimaging in moving individuals. fNIRS might prove useful to experimentally test the notion that visual and inertial information on self-motion perception are merged in the ventral-intraparietal area (e.g., [43, 44]) in humans, and as a tool to monitor, for example, workload and vigilance[24] for humans operating in extreme environments.

5 Acknowledgments

The authors would like to thank Daniel Diers for the development of software used to visualize the fNIRS recording sites (http://www.kyb.tuebingen.mpg.de/research/dep/bu/motion-perception-and-simulation/qvis.html).

References

[1] R. Ratcliff, A theory of memory retrieval., Psychological review 85 (2) (1978) 59.

[2] J. I. Gold, M. N. Shadlen, The neural basis of decision making, Annu. Rev. Neurosci. 30 (2007) 535–574.

[3] J. Drugowitsch, G. C. DeAngelis, E. M. Klier, D. E. Angelaki, A. Pouget, Optimal multisensory decision-making in a reaction-time task, Elife 3 (2014) e03005.

[4] A. Nesti, K. de Winkel, H. H. Bülthoff, Accumulation of inertial sensory information in the perception of whole body yaw rotation, PLoS one 12 (1) (2017) e0170497.

[5] J.-N. Kim, M. N. Shadlen, Neural correlates of a decision in the dorsolateral prefrontal cortex of the macaque, Nature neuroscience 2 (2) (1999) 176–185.

[6] M. N. Shadlen, W. T. Newsome, Neural basis of a perceptual decision in the parietal cortex (area lip) of the rhesus monkey, Journal of neurophysiology 86 (4) (2001) 1916–1936.

[7] R. Kiani, M. N. Shadlen, Representation of confidence associated with a decision by neurons in the parietal cortex, science 324 (5928) (2009) 759–764.

[8] D. Raposo, M. T. Kaufman, A. K. Churchland, A category-free neural population supports evolving demands during decision-making, Nature neuroscience 17 (12) (2014) 1784–1792.

[9] T. D. Hanks, C. D. Kopec, B. W. Brunton, C. A. Duan, J. C. Erlich, C. D. Brody, Distinct relationships of parietal and prefrontal cortices to evidence accumulation, Nature 520 (7546) (2015) 220–223.

[10] S. Kira, T. Yang, M. N. Shadlen, A neural implementation of walds sequential probability ratio test, Neuron 85 (4) (2015) 861–873.

[11] R. G. O'connell, P. M. Dockree, S. P. Kelly, A supramodal accumulation-to-bound signal that determines perceptual decisions in humans, Nature neuroscience 15 (12) (2012) 1729–1735.

[12] S. P. Kelly, R. G. O'Connell, Internal and external influences on the rate of sensory evidence accumulation in the human brain, Journal of Neuroscience 33 (50) (2013) 19434–19441.

[13] I. I. Goncharova, D. J. McFarland, T. M. Vaughan, J. R. Wolpaw, Emg contamination of eeg: spectral and topographical characteristics, Clinical neurophysiology 114 (9) (2003) 1580–1593.

[14] B. Chance, Near-infrared images using continuous, phase-modulated, and pulsed light with quantitation of blood and blood oxygenationa, Annals of the New York Academy of Sciences 838 (1) (1998) 29–45.

[15] M. Izzetoglu, K. Izzetoglu, S. Bunce, H. Ayaz, A. Devaraj, B. Onaral, K. Pourrezaei, Functional near-infrared neuroimaging, IEEE Transactions on Neural Systems and Rehabilitation Engineering 13 (2) (2005) 153–159.

[16] H. Ayaz, P. A. Shewokis, A. Curtin, M. Izzetoglu, K. Izzetoglu, B. Onaral, Using mazesuite and functional near infrared spectroscopy to study learning in spatial navigation, JoVE (Journal of Visualized Experiments) (56) (2011) e3443–e3443.

[17] F. F. Jobsis, Noninvasive, infrared monitoring of cerebral and myocardial oxygen sufficiency and circulatory parameters, Science 198 (4323) (1977) 1264–1267.

[18] G. L. Greig, Masking of motion cues by random motion: comparison of human performance with a signal detection model, Tech. rep., University of Toronto (1988).

[19] L. Zaichik, V. Rodchenko, I. Rufov, Y. Yashin, A. White, Acceleration perception, in: Modeling and Simulation Technologies Conference and Exhibit, 1999, p. 4334.

[20] J. S. Butler, S. T. Smith, J. L. Campos, H. H. Bülthoff, Bayesian integration of visual and vestibular signals for heading, Journal of vision 10 (11) (2010) 23–23.

[21] A. Nesti, K. A. Beykirch, P. R. MacNeilage, M. Barnett-Cowan, H. H. Bülthoff, The importance of stimulus noise analysis for self-motion studies, PloS one 9 (4) (2014) e94570.

[22] R. Oostenveld, P. Praamstra, The five percent electrode system for high-resolution eeg and erp measurements, Clinical neurophysiology 112 (4) (2001) 713–719.

[23] H. Li, J. Ruan, Z. Xie, H. Wang, W. Liu, Investigation of the critical geometric characteristics of living human skulls utilising medical image analysis techniques, International Journal of Vehicle Safety 2 (4) (2007) 345–367.

[24] H. Ayaz, P. A. Shewokis, S. Bunce, K. Izzetoglu, B. Willems, B. Onaral, Optical brain monitoring for operator training and mental workload assessment, Neuroimage 59 (1) (2012) 36–47.

[25] K. De Winkel, F. Soyka, M. Barnett-Cowan, H. Bülthoff, E. Groen, P. Werkhoven, Integration of visual and inertial cues in the perception of angular self-motion, Experimental brain research 231 (2) (2013) 209–218.

[26] F. A. Wichmann, N. J. Hill, The psychometric function: I. fitting, sampling, and goodness of fit, Attention, Perception, & Psychophysics 63 (8) (2001) 1293–1313.

[27] R. A. Fisher, On the mathematical foundations of theoretical statistics, Philosophical Transactions of the Royal Society of London. Series A, Containing Papers of a Mathematical or Physical Character 222 (1922) 309–368.

[28] G. Wilkinson, C. Rogers, Symbolic description of factorial models for analysis of variance, Applied Statistics (1973) 392–399.

[29] S. Luu, T. Chau, Decoding subjective preference from single-trial near-infrared spectroscopy signals, Journal of neural engineering 6 (1) (2008) 016003.

[30] S. A. Huettel, A. W. Song, G. McCarthy, Functional magnetic resonance imaging, Vol. 1, Sinauer Associates Sunderland, 2004.

[31] D. Green, J. Swets, Signal Detection Theory and Psychophysics, John Wiley and Sons, 1966.
URL `https://books.google.de/books?id=yYsQAQAAIAAJ`

[32] D. C. Krawczyk, Contributions of the prefrontal cortex to the neural basis of human decision making, Neuroscience & Biobehavioral Reviews 26 (6) (2002) 631–664.

[33] M. E. Walton, J. T. Devlin, M. F. Rushworth, Interactions between decision making and performance monitoring within prefrontal cortex, Nature neuroscience 7 (11) (2004) 1259–1265.

[34] F. Manes, B. Sahakian, L. Clark, R. Rogers, N. Antoun, M. Aitken, T. Robbins, Decision-making processes following damage to the prefrontal cortex, Brain 125 (3) (2002) 624–639.

[35] M. S. Fleck, S. M. Daselaar, I. G. Dobbins, R. Cabeza, Role of prefrontal and anterior cingulate regions in decision-making processes shared by memory and nonmemory tasks, Cerebral Cortex 16 (11) (2006) 1623–1630.

[36] M. Brand, K. Labudda, H. J. Markowitsch, Neuropsychological correlates of decision-making in ambiguous and risky situations, Neural Networks 19 (8) (2006) 1266–1276.

[37] M. Causse, P. Péran, F. Dehais, C. F. Caravasso, T. Zeffiro, U. Sabatini, J. Pastor, Affective decision making under uncertainty during a plausible aviation task: An fmri study, NeuroImage 71 (2013) 19–29.

[38] S. I. Di Domenico, A. Le, Y. Liu, H. Ayaz, M. A. Fournier, Basic psychological needs and neurophysiological responsiveness to decisional conflict: an event-related potential study of integrative self processes, Cognitive, Affective, & Behavioral Neuroscience 16 (5) (2016) 848–865.

[39] H. Mittelstaedt, M.-L. Mittelstaedt, Homing by path integration, in: Avian navigation, Springer, 1982, pp. 290–297.

[40] A. S. Etienne, K. J. Jeffery, Path integration in mammals, Hippocampus 14 (2) (2004) 180–192.

[41] J. L. Souman, I. Frissen, M. N. Sreenivasa, M. O. Ernst, Walking straight into circles, Current Biology 19 (18) (2009) 1538–1542.

[42] F. H. Petzschner, S. Glasauer, Iterative bayesian estimation as an explanation for range and regression effects: a study on human path integration, Journal of Neuroscience 31 (47) (2011) 17220–17229.

[43] A. Chen, G. C. DeAngelis, D. E. Angelaki, Convergence of vestibular and visual self-motion signals in an area of the posterior sylvian fissure, Journal of Neuroscience 31 (32) (2011) 11617–11627.

[44] A. Chen, G. C. DeAngelis, D. E. Angelaki, Representation of vestibular and visual cues to self-motion in ventral intraparietal cortex, Journal of Neuroscience 31 (33) (2011) 12036–12052.

- Prefrontal and parietal areas are thought to orchestrate decision making
- We investigate whether this applies to decisions on self-motion using fNIRS
- Parietal activity predicts judgments on whole-body yaw rotation intensity
- Results suggest parietal activity reflects modality-independent decision variables